Aerospace Science and Technology 66 (2017) 392–401

Contents lists available at ScienceDirect

Aerospace Science and Technology

www.elsevier.com/locate/aescte

Thermomechanical buckling and post-buckling of cylindrical shell with functionally graded coatings and reinforced by stringers

Pham Toan Thang [a,b,*], Nguyen Dinh Duc [c,d], T. Nguyen-Thoi [a,b]

[a] Division of Computational Mathematics and Engineering, Institute for Computational Science, Ton Duc Thang University, Ho Chi Minh City, Viet Nam
[b] Faculty of Civil Engineering, Ton Duc Thang University, Ho Chi Minh City, Viet Nam
[c] Advanced Materials and Structures Laboratory, VNU-Hanoi, University of Engineering and Technology (UET), 144 Xuan Thuy, Cau Giay, Hanoi, Viet Nam
[d] Infrastructure Engineering Program, VNU-Hanoi, Vietnam–Japan University (VJU), My Dinh 1, Tu Liem, Hanoi, Viet Nam

ARTICLE INFO

Article history:
Received 13 December 2016
Received in revised form 23 February 2017
Accepted 17 March 2017
Available online 21 March 2017

Keywords:
Cylindrical shell
Functionally graded materials
Thermomechanical buckling and post-buckling
Airy stress function

ABSTRACT

The cylindrical shells reinforced by stringers have been widely used in modern engineering structures such as storage tanks, missile, submarine hull, oil-transmitting pipeline, etc. In this present article, the thermomechanical buckling and post-buckling behaviors of a cylindrical shell with functionally graded (FG) coatings are investigated by an analytical approach. The cylindrical shell is reinforced by outside stringers under torsional load in the thermal environment. The layers of FG coatings are assumed to be made by functionally graded materials (FGMS) combining of ceramic and metal phases and the core of the shell is made from homogeneous material. The classical shell theory based on the von-Karman assumptions is used to model the thin cylindrical shell. Using Galerkin's procedure and Airy stress function, the governing equations can be solved to obtain the closed-form solution for the critical buckling load and postbuckling load-deflection curves of simply supported shells. Moreover, many important parametric studies of stringers, temperature field, material volume fraction index, the thickness of metal layer, etc. are taken into investigation. According to numerical examples, it is revealed that the outside strings have considerably impact on thermomechanical buckling and postbuckling behaviors of the shells.

1. Introduction

Due to the development of the materials science, a new type of composite materials known as functionally graded materials (FGMs) has been widely used in various engineering applications, especially in high temperature status. FGMs are produced by a continuous mixture of metal and ceramic in which material properties vary smoothly and continuously in the preferred, generally in the thickness direction [1,2]. The metal gives high roughness while the ceramic provides high temperature-resistance and high corrosion-resistant. The concept of FGM was first introduced by a group of material scientists in Japan in the mid-1980s [3,4]. Since then, many investigations, due to their fascinating features of potential applications, have been carried out to study the mechanical buckling, thermal buckling, and stability of the structures made of FGM.

The cylindrical shell structures, as a type of fundamental structural components, are widely in the engineering applications such as a missile, submarine hull, oil-transmitting pipeline, aircraft, hydrospace, shipbuilding construction [5–11]. For example, the strategic missiles using solid materials, they are capable to fly far beyond the continent with great velocity, so their hull could stand very high strength and high temperatures. To satisfy it, the shell of the strategic missiles is usually made of composite carbon–carbon or FGMs. Furthermore, the functionally graded cylindrical shells could also be used as the shell of a nuclear reactor or special engineering pipes [12]. In practice, this kind of structures is often subjected to the intricate environment and complex loading conditions. Thus, it is of great importance to achieve an insight into thermomechanical buckling behavior of the FG cylindrical shell for the engineers and designers.

In the research fields of cylindrical shells, many studies have been addressed for the mechanical buckling and postbuckling problems as Shen [13–16], Huang et al. [17–20], Sofiyev [21], Dai and Zheng [22], Dai et al. [23], Bagherizadeh et al. [24], Akbari Alashti and Ahmadi [25], Sun et al. [26], Duc et al. [27,28], Thang et al. [29]. Many investigations on analytical and numerical methods have been conducted to analyze the thermal buckling behavior

* Corresponding author at: Division of Computational Mathematics and Engineering, Institute for Computational Science, Ton Duc Thang University, Ho Chi Minh City, Viet Nam.
E-mail address: phamtoanthang@tdt.edu.vn (P.T. Thang).

http://dx.doi.org/10.1016/j.ast.2017.03.023
1270-9638/

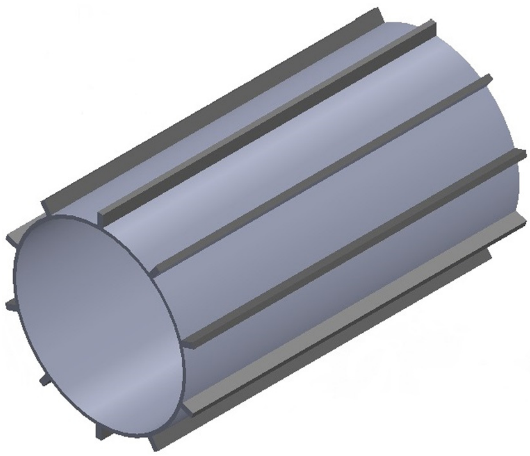

Fig. 1. Configuration of circular cylindrical shell with FG coatings and reinforced by stringers.

of the FG cylindrical shell such as Shahsiah and Eslami [30], Shen [31], Wu et al. [32], Yaghoobi et al. [33], and Thang [34]. An effective meshfree method with highly smoothing shape functions for buckling analysis of Kirchhoff–Love cylindrical was investigated by Wang et al. [35].

For the torsional buckling problem, Li et al. [36] considered a cylindrical crack located in an FGM interlayer between two coaxial elastic dissimilar homogeneous cylinders and subjected to a torsional impact loading. Singh et al. [37] studied the torsional vibrations of functionally graded finite cylinders. Arghavan and Hematiyan [38] presented an analytical formulation for torsional analysis of functionally graded hollow tubes of arbitrary shape. Wang et al. [39] proposed an analytical solution for transient torsional responses of a finitely long, functionally graded hollow cylinder. The torsional impact problem of a cylindrical interface crack between an FGM interlayer and its external homogeneous cylinder was investigated by Feng [40]. Shen [41] also investigated the torsional buckling and postbuckling of FGM cylindrical shells. Najafov et al. [42] examined the torsional vibration and stability problems of FG orthotropic cylindrical shells in the elastic medium. Huang [43] investigated the buckling behaviors of elasto-plastic functionally graded cylindrical shells subjected to torsional load.

Recently, the torsional vibration and buckling analysis of cylindrical shell with FG coatings has been investigated by Sofiyev and Kuruoglu [44]. In this study, the thermomechanical buckling and post-buckling behaviors of cylindrical shells with FG coatings are investigated by analytical approach. The highlight of this study is that the cylindrical shell is reinforced by the outside stringers. Moreover, the cylindrical shells with FG coatings are subjected to torsional load in the thermal environment. The layers of FG coatings are assumed to be made by functionally graded materials (FGMS) combining of ceramic and metal phases and the core of the shell is made from homogeneous material. By using the Galerkin procedure, the closed form expressions can be determined to obtain the critical buckling load and post-buckling response. Several numerical examples are also presented to demonstrate the nonlinear behaviors of cylindrical shell with FG coatings.

For clarity, the content of this research paper is organized as follows: Section 2 presents the configuration of the cylindrical shell with FG coatings and the outside stringers system. Mathematical modeling of the cylindrical shell with FG coatings is analyzed in Section 3. Sections 4 presents the thermomechanical buckling and post-buckling analysis. Several numerical examples are given in Section 5. Finally, the concluding remarks are drawn in Section 6.

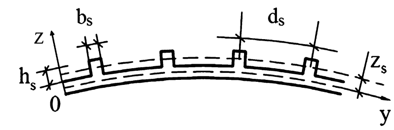

Fig. 2. Coordinate system of axial stiffeners.

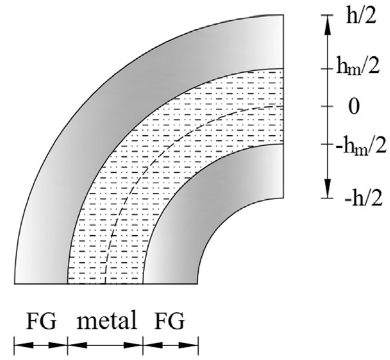

Fig. 3. Configuration for cylindrical shell with FG coatings.

2. Configuration of the cylindrical shell with FG coatings and the stringers

Consider a circular cylindrical shell with FG coatings with mean radius R, length L, and thickness h. The cylindrical shell is reinforced by the outside stringers system as shown in Fig. 1 and Fig. 2. Following the power-law distribution in z-direction, the volume fraction of the metal component, V_m can be determined as [29] (see Fig. 3)

$$V_m(z) = \begin{cases} [\frac{-2|z|+h}{(h-h_m)}]^{\xi}, & -\frac{h}{2} \le z \le -\frac{h_m}{2} \text{ or } \frac{h_m}{2} \le z \le \frac{h}{2}, \\ 1, & -\frac{h_m}{2} \le z \le \frac{h_m}{2}, \end{cases} \tag{1}$$

where ξ is the volume fraction exponent which dictates the material variation profile through the thickness of the shell. The non-homogeneous material properties of cylindrical shell with FG coating are obtained by the rule of mixture as follows:

$$P = P_{mc} V_c(z) + P_c \tag{2}$$

in which $P_{mc} = P_m - P_c$ and P_m, P_c are the thermomechanical properties of the metal and ceramic, respectively. In order to accurately analysis the thermomechanical characteristics of the shell, the temperature dependency of material constituents is taken into account as [31]

$$P(T) = P_0\big(P_{-1}T^{-1} + 1 + P_1T^1 + P_2T^2 + P_3T^3\big), \tag{3}$$

where P_0, P_{-1}, P_1, P_2, and P_3 are the coefficients of temperature T and unique to the constituent materials, and T_0 is the room temperature.

3. Mathematical modeling

According to the classical shell theory with Kirchhoff assumptions, the displacement components of a shell is written as [45,46]

$$\begin{aligned} U(x, y, z) &= u(x, y) - z\frac{\partial w(x, y)}{\partial x}, \\ U(x, y, z) &= v(x, y) - z\frac{\partial w(x, y)}{\partial y}, \\ W(x, y, z) &= w(x, y), \end{aligned} \tag{4}$$

where (u, v, w) are the displacement components along the (x, y, z) coordinates directions, respectively, of a point on the mid-plane (i.e., $z = 0$).

The von-Karman nonlinear strain-displacement relations can be expressed as follows [46]

$$\begin{Bmatrix} \varepsilon_x \\ \varepsilon_y \\ \gamma_{xy} \end{Bmatrix} = \begin{Bmatrix} \varepsilon_x^0 \\ \varepsilon_y^0 \\ \gamma_{xy}^0 \end{Bmatrix} + z \begin{Bmatrix} \kappa_x \\ \kappa_y \\ \kappa_{xy} \end{Bmatrix} \tag{5}$$

where

$$\begin{Bmatrix} \varepsilon_x^0 \\ \varepsilon_y^0 \\ \gamma_{xy}^0 \end{Bmatrix} = \begin{Bmatrix} \frac{\partial u}{\partial x} + \frac{1}{2}(\frac{\partial w}{\partial x})^2 \\ \frac{\partial v}{\partial y} - \frac{w}{R} + \frac{1}{2}(\frac{\partial w}{\partial y})^2 \\ \frac{\partial u}{\partial y} + \frac{\partial v}{\partial x} + \frac{\partial w}{\partial x}\frac{\partial w}{\partial y} \end{Bmatrix},$$

$$\begin{Bmatrix} \kappa_x \\ \kappa_y \\ \kappa_{xy} \end{Bmatrix} = \begin{Bmatrix} -\frac{\partial^2 w}{\partial x^2} \\ -\frac{\partial^2 w}{\partial y^2} \\ -2\frac{\partial^2 w}{\partial x \partial y} \end{Bmatrix} \tag{6}$$

where ε_x, ε_y and γ_{xy} are normal and shearing strain components at any point the shell thickness, and $\varepsilon_{x0}, \varepsilon_{y0}$ and γ_{xy0} are denoted as the corresponding quantities at points on the shell middle surface only, $\kappa_x, \kappa_y, \kappa_{xy}$ are the flexural strains.

The linear constitutive relations for the cylindrical shell with FG coatings are given by [45,46]

$$\begin{Bmatrix} \sigma_x^{sh} \\ \sigma_y^{sh} \\ \sigma_{xy}^{sh} \end{Bmatrix} = \begin{bmatrix} Q_{11}^{sh} & Q_{12}^{sh} & 0 \\ Q_{12}^{sh} & Q_{22}^{sh} & 0 \\ 0 & 0 & Q_{66}^{sh} \end{bmatrix} \begin{Bmatrix} \varepsilon_x - \alpha^{sh}\Delta T \\ \varepsilon_y - \alpha^{sh}\Delta T \\ \gamma_{xy} \end{Bmatrix}, \tag{7}$$

where

$$Q_{11}^{sh} = Q_{22}^{sh} = \frac{E_{sh}(z,T)}{1-\nu^2}, \qquad Q_{12}^{sh} = \frac{\nu E_{sh}(z,T)}{1-\nu^2},$$
$$Q_{66}^{sh} = \frac{E_{sh}(z,T)}{2(1+\nu)}, \tag{8}$$

and for the stringers

$$\sigma_x^{st} = E^{st}\varepsilon_x - E^{st}\alpha^{st}\Delta T \tag{9}$$

in which, (E^{sh}, E^{st}) and $(\alpha^{sh}, \alpha^{st})$ are Young's modulus, thermal expansion coefficient of the shell and the stringers, respectively; ΔT is the temperature change. In this study, we assume that $E^{st} = E_c(T)$, $\alpha^{st} = \alpha_c(T)$.

Using the smeared technique and omitting the twist of stiffeners, the force and moment of cylindrical shell reinforced by the stringers can be determined as follows [47]

$$N_x = \int_{-h/2}^{h/2} \sigma_x^{sh} dz + \int_{h/2}^{h/2+h_{st}} \sigma_x^{st} \frac{b_s}{d_s} dz,$$

$$N_y = \int_{-h/2}^{h/2} \sigma_y^{sh} dz, \qquad N_{xy} = \int_{-h/2}^{h/2} \sigma_{xy} dz,$$

$$M_x = \int_{-h/2}^{h/2} \sigma_x^{sh} z dz + \int_{h/2}^{h/2+h_{st}} \sigma_x^{st} \frac{b_s}{d_s} z dz,$$

$$M_y = \int_{-h/2}^{h/2} \sigma_y^{sh} z dz, \qquad M_{xy} = \int_{-h/2}^{h/2} \sigma_{xy}^{sh} z dz. \tag{10}$$

Substituting Eqs. (5)–(6) into Eqs. (7) and (9) and then into Eq. (10), leads to

$$\begin{Bmatrix} N_x \\ N_y \\ N_{xy} \\ M_x \\ M_y \\ M_{xy} \end{Bmatrix} = \begin{bmatrix} A_{11} & A_{12} & 0 & B_{11} & B_{12} & 0 \\ A_{12} & A_{22} & 0 & B_{12} & B_{22} & 0 \\ 0 & 0 & A_{66} & 0 & 0 & B_{66} \\ B_{11} & B_{12} & 0 & D_{11} & D_{12} & 0 \\ B_{12} & B_{22} & 0 & D_{12} & D_{22} & 0 \\ 0 & 0 & B_{66} & 0 & 0 & D_{66} \end{bmatrix} \begin{Bmatrix} \varepsilon_x^0 \\ \varepsilon_y^0 \\ \gamma_{xy}^0 \\ \kappa_x \\ \kappa_y \\ \kappa_{xy} \end{Bmatrix} - \begin{Bmatrix} \Phi_1 + \Phi_{1s} \\ \Phi_1 \\ 0 \\ \Phi_2 + \Phi_{2s} \\ \Phi_2 \\ 0 \end{Bmatrix} \tag{11}$$

where, the mathematical expressions of stringers coefficient A_{ij} $(i = 1 \div 6,\ j = 1 \div 4)$ and thermal coefficients $\Phi_1, \Phi_2, \Phi_{1s}, \Phi_{2s}$ are given by

$$A_{11} = \frac{E_1}{1-\nu^2} + \frac{E_{1s}b_s}{d_s}, \qquad A_{12} = \frac{\nu E_1}{1-\nu^2}, \qquad A_{22} = \frac{E_1}{1-\nu^2},$$
$$A_{66} = \frac{E_1}{2(1+\nu)}$$
$$B_{11} = \frac{E_2}{1-\nu^2} + \frac{E_{2s}b_s}{d_s}, \qquad B_{12} = \frac{\nu E_2}{1-\nu^2}, \qquad B_{22} = \frac{E_2}{1-\nu^2},$$
$$B_{66} = \frac{E_2}{2(1+\nu)}$$
$$D_{11} = \frac{E_3}{1-\nu^2} + \frac{E_{3s}b_s}{d_s}, \qquad D_{12} = \frac{\nu E_3}{1-\nu^2}, \qquad D_{22} = \frac{E_3}{1-\nu^2},$$
$$D_{66} = \frac{E_3}{2(1+\nu)} \tag{12}$$

in which

$$E_1 = \int_{-h/2}^{h/2} E^{sh}(z) dz, \qquad E_2 = \int_{-h/2}^{h/2} E^{sh}(z) z dz,$$

$$E_3 = \int_{-h/2}^{h/2} E^{sh}(z) z^2 dz$$

$$E_{1s} = \int_{h/2}^{h/2+h_m} E^s(z) dz, \qquad E_{2s} = \int_{h/2}^{h/2+h_m} E^s(z) z dz,$$

$$E_{3s} = \int_{h/2}^{h/2+h_m} E^s(z) z^2 dz,$$

$$\Phi_1 = \int_{-h/2}^{h/2} E^{sh}(z)\alpha^{sh}(z)\Delta T dz,$$

$$\Phi_2 = \int_{-h/2}^{h/2} E^{sh}(z)\alpha^{sh}(z)\Delta T z dz,$$

$$\Phi_{1s} = \frac{b_s}{d_s}\int_{h/2}^{h/2+h_s} E^s\alpha^s\Delta T dz, \qquad \Phi_{2s} = \frac{b_s}{d_s}\int_{h/2}^{h/2+h_s} E^s\alpha^s\Delta T dz \tag{13}$$

From Eq. (11), we have

$$\varepsilon_x^0 = A_{11}^* N_x - A_{12}^* N_y + A_{13}^* \kappa_x + A_{14}^* \kappa_y + A_{15}^* \Phi_1 + A_{11}^* \Phi_{1s},$$
$$\varepsilon_y^0 = -A_{12}^* N_x + A_{22}^* N_y + A_{23}^* \kappa_x + A_{24}^* \kappa_y + A_{25}^* \Phi_1 - A_{12}^* \Phi_{1s},$$
$$\gamma_{xy}^0 = A_{31}^* N_{xy} - A_{32}^* \kappa_{xy}, \tag{14}$$

where

$$A_{11}^* = \frac{A_{22}}{A_{11}A_{22} - A_{12}^2}, \qquad A_{12}^* = \frac{A_{12}}{A_{11}A_{22} - A_{12}^2},$$
$$A_{13}^* = \frac{A_{12}B_{12} - A_{22}B_{11}}{A_{11}A_{22} - A_{12}^2},$$
$$A_{14}^* = \frac{A_{12}B_{22} - A_{22}B_{12}}{A_{11}A_{22} - A_{12}^2}, \qquad A_{15}^* = \frac{A_{22} - A_{12}}{A_{11}A_{22} - A_{12}^2},$$
$$A_{22}^* = \frac{A_{11}}{A_{11}A_{22} - A_{12}^2}$$
$$A_{23}^* = \frac{A_{12}B_{11} - A_{11}B_{12}}{A_{11}A_{22} - A_{12}^2}, \qquad A_{24}^* = \frac{A_{12}B_{12} - A_{11}B_{22}}{A_{11}A_{22} - A_{12}^2},$$
$$A_{25}^* = \frac{A_{11} - A_{12}}{A_{11}A_{22} - A_{12}^2}, \qquad A_{31}^* = \frac{1}{A_{66}}, \qquad A_{32}^* = \frac{B_{66}}{A_{66}} \tag{15}$$

Substituting once again Eq. (14) into M_x, M_y and M_{xy} in Eq. (11), leads to

$$M_x = B_{11}^* N_x + B_{12}^* N_y + B_{13}^* \kappa_x + B_{14}^* \kappa_y + B_{15}^* \Phi_1 + B_{11}^* \Phi_{1s} - \Phi_2,$$
$$M_y = B_{21}^* N_x + B_{22}^* N_y + B_{23}^* \kappa_x + B_{24}^* \kappa_y + B_{25}^* \Phi_1 + B_{21}^* \Phi_{1s} - \Phi_2,$$
$$M_{xy} = B_{31}^* N_{xy} + B_{32}^* \kappa_{xy}, \tag{16}$$

where

$$B_{11}^* = B_{11}A_{11}^* - B_{12}A_{12}^*, \qquad B_{12}^* = B_{12}A_{22}^* - B_{11}A_{12}^*,$$
$$B_{13}^* = D_{11} + B_{12}A_{23}^* + B_{11}A_{13}^*,$$
$$B_{14}^* = D_{12} + B_{11}A_{14}^* + B_{12}A_{24}^*$$
$$B_{15}^* = B_{11}A_{15}^* + B_{12}A_{25}^*, \qquad B_{21}^* = B_{12}A_{11}^* - B_{22}A_{12}^*,$$
$$B_{22}^* = B_{22}A_{22}^* - B_{12}A_{12}^*, \qquad B_{23}^* = D_{12} + B_{12}A_{13}^* + B_{22}A_{23}^*$$
$$B_{24}^* = D_{22} + B_{12}A_{14}^* + B_{22}A_{24}^*, \qquad B_{15}^* = B_{12}A_{15}^* + B_{22}A_{25}^*$$
$$B_{31}^* = B_{66}A_{31}^*, \qquad B_{32}^* = D_{66} - B_{66}A_{32}^*. \tag{17}$$

The nonlinear equilibrium equations of cylindrical shell with FG coatings based on the CST are given by [45]:

$$\frac{\partial N_x}{\partial x} + \frac{\partial N_{xy}}{\partial y} = 0, \tag{18a}$$
$$\frac{\partial N_{xy}}{\partial x} + \frac{\partial N_y}{\partial y} = 0 \tag{18b}$$
$$\frac{\partial^2 M_x}{\partial x^2} + 2\frac{\partial^2 M_{xy}}{\partial x \partial y} + \frac{\partial^2 M_y}{\partial y^2} + N_x \frac{\partial^2 w}{\partial x^2} + 2N_{xy}\frac{\partial^2 w}{\partial x \partial y} + N_y \frac{\partial^2 w}{\partial y^2} + \frac{N_x}{R} = 0. \tag{18c}$$

To satisfy the first and second equilibrium equations, a stress function, $F(x, y)$, introduced by G.B. Airy with the following definition is used as [27,48]

$$N_x = \frac{\partial^2 F(x,y)}{\partial y^2}, \qquad N_y = \frac{\partial^2 F(x,y)}{\partial x^2}, \qquad N_{xy} = -\frac{\partial^2 F(x,y)}{\partial x \partial y} \tag{19}$$

Substituting Eqs. (16) and (19) into Eq. (18c), we have

$$C_1^* \frac{\partial^4 w}{\partial x^4} + C_2^* \frac{\partial^4 w}{\partial x^2 \partial y^2} + C_3^* \frac{\partial^4 w}{\partial y^4} + C_4^* \frac{\partial^4 F(x,y)}{\partial x^4} + C_5^* \frac{\partial^4 F(x,y)}{\partial x^2 \partial y^2} + C_6^* \frac{\partial^4 F(x,y)}{\partial y^4} + \frac{\partial^2 w}{\partial x^2}\frac{\partial^2 F(x,y)}{\partial y^2} - 2\frac{\partial^2 w}{\partial x \partial y}\frac{\partial^2 F}{\partial x \partial y} + \frac{\partial^2 w}{\partial y^2}\frac{\partial^2 F(x,y)}{\partial x^2} + \frac{1}{R}\frac{\partial^2 F(x,y)}{\partial x^2} = 0, \tag{20}$$

where

$$C_1^* = -B_{13}^*, \qquad C_2^* = -\left(B_{14}^* + 2B_{32}^* + B_{23}^*\right), \qquad C_3^* = -B_{24}^*,$$
$$C_4^* = B_{12}^*, \qquad C_5^* = \left(B_{11}^* - 2B_{31}^* + B_{22}^*\right), \qquad C_6^* = B_{21}^*. \tag{21}$$

The geometrical compatibility equation for the cylindrical shell can be written as [27,48]

$$\frac{\partial^2 \varepsilon_x^0}{\partial y^2} + \frac{\partial^2 \varepsilon_y^0}{\partial x^2} - \frac{\partial^2 \gamma_{xy}^0}{\partial x \partial y} = \left(\frac{\partial^2 w}{\partial x \partial y}\right)^2 - \frac{\partial^2 w}{\partial x^2}\frac{\partial^2 w}{\partial y^2} - \frac{1}{R}\frac{\partial^2 w}{\partial x^2}. \tag{22}$$

The compatibility equation of a circular cylindrical shell with FG coatings in terms of the Airy stress function $F(x, y)$ and displacement component w may be obtained by substituting Eqs. (14) and (19) into Eq. (22), leads to

$$D_1^* \frac{\partial^4 F(x,y)}{\partial x^4} + D_2^* \frac{\partial^4 F(x,y)}{\partial x^2 \partial y^2} + D_3^* \frac{\partial^4 F(x,y)}{\partial y^4} + D_4^* \frac{\partial^4 w}{\partial x^4} + D_5^* \frac{\partial^4 w}{\partial x^2 \partial y^2} + D_6^* \frac{\partial^4 w}{\partial y^4} - \left(\frac{\partial^2 w}{\partial x \partial y}\right)^2 + \frac{\partial^2 w}{\partial x^2}\frac{\partial^2 w}{\partial y^2} + \frac{1}{R}\frac{\partial^2 w}{\partial x^2} = 0, \tag{23}$$

where

$$D_1^* = -A_{22}^*, \qquad D_2^* = A_{31}^* - 2A_{12}^*, \qquad D_3^* = A_{11}^*,$$
$$D_4^* = -A_{23}^*, \qquad D_5^* = -\left(A_{13}^* + A_{24}^* + A_{32}^*\right), \qquad D_6^* = -A_{15}^*. \tag{24}$$

Eqs. (20) and (24) are the nonlinear governing equations used to investigate the thermomechanical buckling and post-buckling behaviors of the cylindrical shell with FG coatings under torsional load.

4. Stability analysis

4.1. Solution and boundary condition

Consider a circular cylindrical shell with FG coatings and it is simply supported at two butt-ends $x = 0$ and $x = L$. In this case, the deflection of the cylindrical shell can be expressed as [49]

$$w = W_0 + W_1 \sin(\alpha x)\sin\left[\beta(y - \kappa x)\right] + W_2 \sin^2(\alpha x) \tag{25}$$

in which

$$\alpha = m\pi/L, \quad m = 1, 2, 3, \ldots$$
$$\beta = n/R, \quad n = 1, 2, 3, \ldots \tag{26}$$

where m, n are the numbers of axis half waves in x and y, respectively. The first term of the deflection in Eq. (25) represents the uniform deflection of points belonging to two butt-ends $x = 0$ and $x = L$, the second term is the linear buckling shape, and third term is the nonlinear buckling shape of the shell.

Setting of Eq. (25) into Eq. (24), leads to

$$D_1^*\frac{\partial^4 F(x,y)}{\partial x^4}+D_2^*\frac{\partial^4 F(x,y)}{\partial x^2\partial y^2}+D_3^*\frac{\partial^4 F(x,y)}{\partial y^4}$$
$$=K_1^*\cos 2\alpha x+K_2^*\cos 2\beta(y-\kappa x)$$
$$+K_3^*\cos\beta\left[y+\left(\frac{\alpha}{\beta}-\kappa\right)x\right]$$
$$+K_4^*\cos\beta\left[y-\left(\frac{\alpha}{\beta}+\kappa\right)x\right]+K_5^*\left\{\cos\beta\left[y-\left(3\frac{\alpha}{\beta}+\kappa\right)x\right]\right.$$
$$\left.-\cos\beta\left[y+\left(3\frac{\alpha}{\beta}-\kappa\right)x\right]\right\}, \tag{27}$$

$$K_1^*=2\alpha^2\left(4D_4^*\alpha^2-\frac{1}{R}\right)W_2+\frac{1}{2}\alpha^2\beta^2W_1^2,$$
$$K_2^*=\frac{1}{2}\alpha^2\beta^2W_1^2,$$
$$K_3^*=\frac{1}{2}D_4^*\left[\left(\alpha^2+\kappa^2\beta^2\right)^2+(2\kappa\alpha\beta)^2\right]W_1$$
$$-\frac{1}{2}\left(\frac{1}{R}-D_5^*\beta^2\right)\left(\alpha^2+\kappa^2\beta^2\right)W_1+\frac{1}{2}D_6^*\beta^4W_1$$
$$+\left[-2D_4^*\left(\alpha^2+\kappa^2\beta^2\right)+\frac{1}{R}-D_5^*\beta^2\right]\kappa\alpha\beta W_1$$
$$+\frac{1}{2}\alpha^2\beta^2W_1W_2,$$
$$K_4^*=-\frac{1}{2}D_4^*\left[\left(\alpha^2+\kappa^2\beta^2\right)^2+(2\kappa\alpha\beta)^2\right]W_1$$
$$+\frac{1}{2}\left(\frac{1}{R}-D_5^*\beta^2\right)\left(\alpha^2+\kappa^2\beta^2\right)W_1-\frac{1}{2}D_6^*\beta^4W_1$$
$$+\left[-2D_4^*\left(\alpha^2+\kappa^2\beta^2\right)+\frac{1}{R}-D_5^*\beta^2\right]\kappa\alpha\beta W_1$$
$$-\frac{1}{2}\alpha^2\beta^2W_1W_2,$$
$$K_5^*=\frac{1}{2}W_1W_2\alpha^2\beta^2. \tag{28}$$

From Eq. (27), the stress function can be determined as follows:

$$F(x,y)=F_1\cos(2\alpha x)+F_1\cos\left[2\beta(y-\kappa x)\right]$$
$$+F_3\cos\left[\beta\left(y+\left(\frac{\alpha}{\beta}-\kappa\right)x\right)\right]$$
$$+F_4\cos\left[\beta\left(y-\left(\frac{\alpha}{\beta}+\kappa\right)x\right)\right]$$
$$+F_5\cos\left[\beta\left(y-\left(3\frac{\alpha}{\beta}+\kappa\right)x\right)\right]$$
$$+F_6\cos\left[\beta\left(y+\left(3\frac{\alpha}{\beta}-\kappa\right)x\right)\right]-Phxy, \tag{29}$$

where P is torsional load intensity, and the coefficients F_i $(i=1\div 6)$ are determined as shown in Appendix A.

In order to establish the closed-form solution for critical buckling load and postbuckling response, the resulting equations can be solved by Galerkin method. First of all, introducing w and f into the left side of Eq. (20), and then applying Galerkin procedure by the way as: Multiplication of two side of Eq. (20) with the form of functions as in Eq. (25), then integrating in the ranges by $0\le y\le 2\pi R$ and $0\le x\le L$, leads to

$$J_1^*+J_2^*W_2+J_3^*W_1^2+J_4^*W_2^2+2Ph\beta^2=0, \tag{30}$$
$$J_5^*W_2-J_6^*W_1^2+J_7^*W_2W_1^2=0, \tag{31}$$

Table 1
Comparison of values of torsional buckling load P_{cr} (MPa) of FGM cylindrical shell without stiffeners.

R/h	Huang and Han [49]	Sofiyev and Kuruoglu [44]	Present
200	81.70 (10, 0.37)	83.67 (8, 0.24)	83.76 (8, 0.37)[a]
300	48.61 (11, 0.33)	49.86 (9, 0.22)	49.88 (9, 0.33)
400	33.82 (12, 0.31)	34.44 (10, 0.21)	35.01 (10, 0.21)
500	25.58 (13, 0.30)	25.93 (11, 0.20)	26.22 (13, 0.30)

[a] The number in the parentheses denote the buckling mode (n,κ), $m=1$.

in which the coefficients J_k^* $(k=1\div 7)$ are determined as in Appendix B.

4.2. The maximal deflection and critical buckling analysis

From Eqs. (30) and (31), the cylindrical shell must also satisfy the circumferential closed condition as [49]

$$\int_0^{2\pi R}\int_0^L\frac{\partial v}{\partial y}\mathrm{d}x\mathrm{d}y=\int_0^{2\pi R}\int_0^L\left[\varepsilon_y^0+\frac{w}{R}-\frac{1}{2}\left(\frac{\partial w}{\partial y}\right)^2\right]\mathrm{d}x\mathrm{d}y=0. \tag{32}$$

Using the Eqs. (14), (19) and (25), Eq. (32) becomes

$$8W_0+4W_2-RW_1^2\beta^2+8R\left(A_{25}^*\Phi_1-A_{12}^*\Phi_{1s}\right)=0. \tag{33}$$

The maximal deflection of the cylindrical shell with FG coatings is defined from Eq. (25) as

$$W_{\max}=W_0+W_1+W_2, \tag{34}$$

here $w=W_{\max}$ locates at $x=\frac{iL}{2m}$, $y=\frac{j\pi R}{2n}+\frac{i\kappa L}{2m}$ in which i,j are old integer numbers.

Solving W_0 from Eq. (33) with respect to W_1 and W_2, and then replacing them into Eq. (34), leads to

$$W_{\max}=-R\left(A_{25}^*\Phi_1-A_{12}^*\Phi_{1s}\right)-\frac{1}{8}RW_1^2\beta^2$$
$$+W_1+\frac{J_6^*W_1^2}{2(J_5^*+J_7^*W_1^2)}. \tag{35}$$

Eliminating W_0 and W_2 from Eqs. (30), (31) and (33), and then solving P with respect to W_1, the closed-form expression can be determined as follows

$$P=-\frac{1}{2h\kappa\beta^2}\left\{J_1^*+\frac{J_6^*J_2^*W_1^2}{(J_5^*+J_7^*W_1^2)}\right.$$
$$\left.+J_3^*W_1^2+\left(\frac{J_6^*J_4^*W_1^2}{(J_5^*+J_7^*W_1^2)}\right)^2\right\}. \tag{36}$$

Note that if $W_1\to 0$ then Eq. (36) leads to

$$P=-\frac{J_1^*}{2h\kappa\beta^2}. \tag{37}$$

Eq. (37) is the explicit expression used to determine critical upper torsional loads for the circular cylindrical shell FG with coatings and reinforced by stringers in the thermal environment.

5. Results and discussion

5.1. Comparative study

In order to validate the results of present formulation, several comparison studies are carried out in Table 1. In this table, the present formulation is compared with those reported by Sofiyev and Kuruoglu [44] and Huang and Han [49] for torsional buckling behavior of functionally graded cylindrical shells. The effect of the stiffeners and temperature field is not considered.

Table 2
Temperature-dependent coefficients of the constituent materials of the considered cylindrical shell with FG coatings [50,51].

Material	Properties	M_0	M_{-1}	M_1	M_2	M_3
(Ceramic)	E (Pa)	3.48E+11	0	−3.70E−04	2.16E−07	−8.95E−11
Si_3N_4	ρ (kg/m^3)	2370	0	0	0	0
	α (K^{-1})	5.87E−06	0	9.10−4	0	0
(Metal)	E (Pa)	2.01E+11	0	3.08E−04	−6.53E−07	0
$SUS304$	ρ (kg/m^3)	8166	0	0	0	0
	α (K^{-1})	1.23E−05	0	8.09E−04	0	0

Table 3
Effect of number of stiffeners and temperature on upper torsional load P (Pa) of cylindrical shell with FG coatings with $L = 2R$, $R/h = 100$, $m = 1$, $n = 8$, $\xi = 1.0$, $h_m = h/4$.

ΔT (K)	$n_s = 20$	$n_s = 15$	$n_s = 10$	$n_s = 5$	$n_s = 0$
0	5.718E+08	5.319E+08	4.958E+08	4.6300E+08	4.331E+08
100	5.599E+08	5.210E+08	4.841E+08	4.515E+08	4.217E+08
300	5.352E+08	4.958E+08	4.598E+08	4.275E+08	3.982E+08
600	4.924E+08	4.528E+08	4.176E+08	3.861E+08	3.575E+08
900	4.369E+08	3.976E+08	3.631E+08	3.324E+08	3.050E+08
1200	3.617E+08	3.220E+08	2.893E+08	2.602E+08	2.343E+08
1500	2.578E+08	2.196E+08	1.882E+08	1.616E+08	1.385E+08

Table 4
Effect of thickness of the metal layer and temperature on upper torsional load P (Pa) of the cylindrical shell with FG coatings with $L = 2R$, $R/h = 100$, $m = 1$, $n = 8$, $\xi = 2.0$, $n_s = 15$.

ΔT (K)	$h_m = 0$	$h_m = 5$	$h_m = h/4$	$h_m = h/3$	$h_m = h/2$
0	3.506E+08	4.167E+08	4.378E+08	4.708E+08	5.147E+08
100	3.487E+08	4.097E+08	4.293E+08	4.592E+08	4.937E+08
300	3.376E+08	3.916E+08	4.090E+08	4.350E+08	4.582E+08
600	3.017E+08	3.522E+08	3.684E+08	3.928E+08	4.161E+08
900	2.404E+08	2.937E+08	3.108E+08	3.379E+08	3.795E+08
1200	1.517E+08	2.111E+08	2.300E+08	2.632E+08	3.394E+08
1500	3.500E+07	9.610E+07	1.173E+08	1.599E+08	2.871E+08

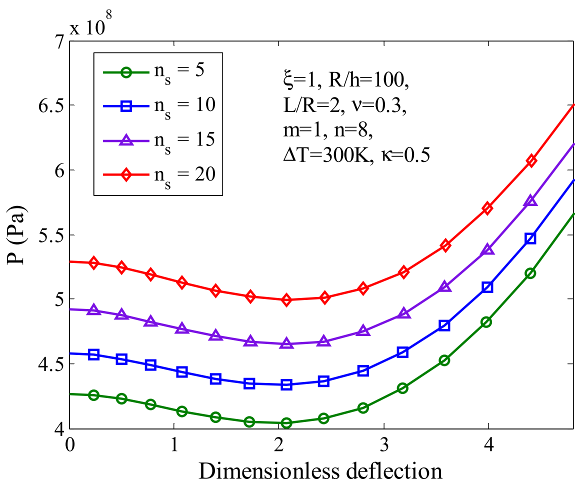

Fig. 4. Effect of number of stiffeners n_s on P (Pa) $- W_{\max}/h$ curves.

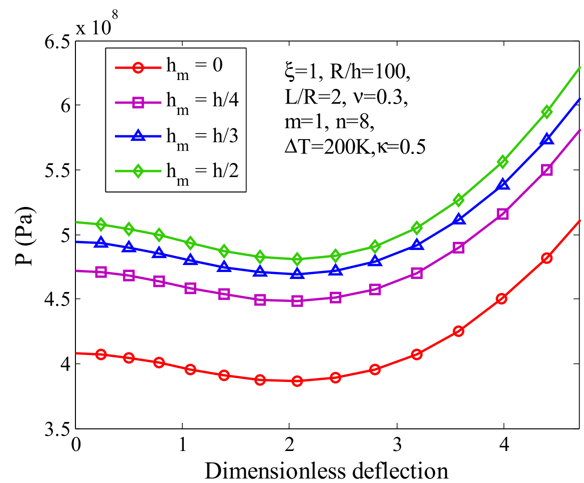

Fig. 5. Effect of h_m on P (Pa) $- W_{\max}/h$ curves.

The geometrical parameters are chosen as $h = 0.01$ m, $L = 2R$. The volume fraction index is taken to be 1. The material properties of the ZrO_2/Ti-6Al-4V cylindrical shell are considered: $E_m = 1.05698 \times 10^{11}$ (Pa), $\nu_m = 0.298099$, $E_c = 1.68063 \times 10^{11}$ (Pa) and $\nu_c = 0.297996$. As observed from Table 1, these comparisons are well-justified.

5.2. Results for buckling and post-buckling of cylindrical shell with FG coatings

After validating the numerical results of present work with the available data in the open literature, some parametric studies are conducted in this subsection. Typical values for Young's modulus E, and the coefficient of thermal expansion α are listed in Table 2.

Firstly, Table 3 shows the effects of number of stiffeners and temperature on upper torsional load P (Pa) of the cylindrical shell with the FG coatings. The shell has $L = 2R$, $R/h = 100$, $h_m = h/4$, the number of stiffener (n_s) is taken to be 0, 5, 10, 15 and 20. The volume fraction index of FG shell is assumed to be constant, $\xi = 1.0$. It can be seen that the maximum torsional load (P) corresponds with $\Delta T = 0$, and $n_s = 20$, and the minimum one is corresponded to $\Delta T = 1500$ K, and $n_s = 0$. Moreover, the results confirm the buckling loads are reduced with increase in temperature. Fig. 4 demonstrates the post-buckling load (P) versus dimensionless deflection $(W_{\max}/h)$ for various of the number of stiffeners. Four different values of parameter of stiffeners (n_s) are considered as 5, 10, 15 and 20. It is observed that by the increasing the number of stiffeners, the torsional load of the cylindrical shell with FG coatings is increased. The prime reason is that the presence of stiffener makes the shells to become stiffer.

In order to demonstrate the effect of the metal layer (h_m), a parametric study has been carried out in Table 4 and Fig. 5. For these examples, the thin cylindrical shell has $L = 2R$, $R/h = 100$. The volume fraction index ξ is taken to be 1. Table 4 presents the buckling load for the thin cylindrical shell with FG coatings under torsional load with the different values of h_m. In this table, the different values of temperature parameter ΔT $(= 0$ K, 100 K, 300 K, 600 K, 900 K, 1200 K, 1400 K) are considered. In can be found that the buckling loads are decreased with increasing in temperature from $\Delta T = 0$ K to $\Delta T = 1500$ K under the same metal layer h_m. In addition, Fig. 5 shows the postbuckling load-deflection curves $(P$ (Pa) $- W_{\max}/h)$ for the cylindrical shell with FG coatings for the different values of h_m at $\Delta T = 300$ (K).

Table 5
Effect of the volume fraction index ξ and temperature on upper torsional load P (Pa) of the cylindrical shell with FG coatings with $R/h = 100$, $L = 2R$, $m = 1$, $n = 8$, $h_m = h/4$, $n_s = 15$.

ΔT (K)	$\xi = 0$	$\xi = 1$	$\xi = 2.0$	$\xi = 3.0$	$\xi = 5.0$	$\xi = 10.0$
0	5.573E+8	4.630E+8	4.378E+8	4.288E+8	4.213E+8	4.187E+8
300	4.972E+8	4.275E+8	4.090E+8	4.018E+8	3.969E+8	3.950E+8
600	4.524E+8	3.860E+8	3.684E+8	3.615E+8	3.568E+8	3.551E+8
900	4.135E+8	3.322E+8	3.108E+8	3.023E+8	2.965E+8	2.943E+8
1200	3.708E+8	2.602E+8	2.310E+8	2.182E+8	2.101E+8	2.071E+8

Table 6
Effect of radius-to-thickness ratio R/h and temperature on upper torsional load P (Pa) of the cylindrical shell with FG coatings with $L = 2R$, $m = 1$, $n = 8$, $\xi = 2.0$, $n_s = 15$.

ΔT (K)		$R/h = 80$	$R/h = 100$	$R/h = 120$	$R/h = 140$	$R/h = 160$
0	$L/R = 1$	6.470E+08	6.241E+08	6.188E+06	6.182E+08	6.176E+08
	$L/R = 2$	4.554E+08	4.505E+08	4.445E+08	4.378E+08	4.340E+08
500	$L/R = 1$	5.717E+08	5.493E+08	5.345E+08	5.310E+08	5.291E+08
	$L/R = 2$	4.030E+08	3.977E+08	3.911E+08	3.835E+08	3.783E+08
1000	$L/R = 1$	4.292E+08	4.271E+08	4.258E+08	4.233E+08	4.212E+08
	$L/R = 2$	3.129E+08	3.062E+08	2.976E+08	2.868E+08	2.753E+08

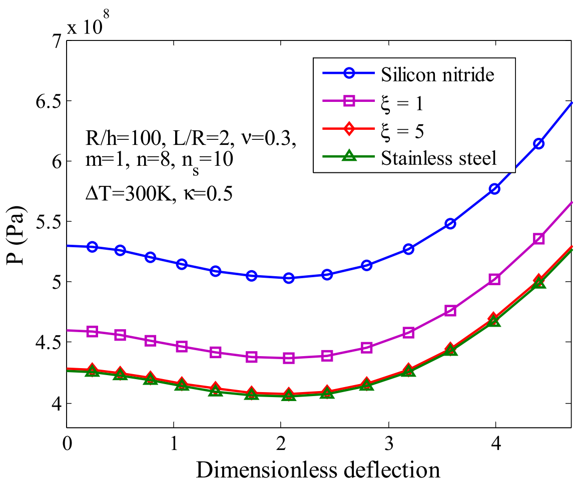

Fig. 6. Effect of volume fraction index ξ on P (Pa) $- W_{\max}/h$ curves.

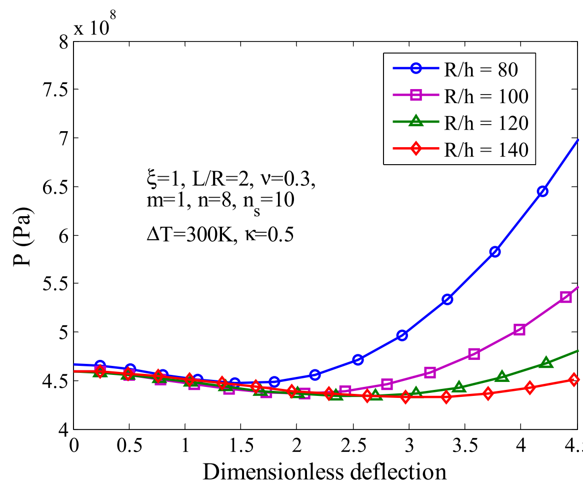

Fig. 7. Effect of R/h ratio on P (Pa) $- W_{\max}/h$ curves.

As it can be observed that the curves are significantly influenced by the metal layer h_m.

Table 5 and Fig. 6 illustrate the buckling load, P (Pa) and load-deflection curves, $P\ (\text{Pa}) - W_{\max}/h$ for simply supported cylindrical shell with FG coatings against the power law index ξ. From Table 5, it is clearly that a fully silicon nitride shell ($\xi = 0$) has highest load parameter. Moreover, it can be also seen that the shell has lower load capacity when the volume fraction index changes from 0 to 10. This is understandable because the ceramic shell is the ones with the higher stiffness than the metal shell.

Next, to examine the influence of radius-to-thickness ratio R/h, as one of important geometrical parameters of the shell, Table 6 shows the variation of torsional load P (Pa) of the cylindrical shell with the various temperature parameter and R/h ratio ranging from 100 to 250. The volume fraction index is taken to be 1. It can be found that the load capacity of the shell is significantly influenced by ratio (R/h). The effect of the radius-to-thickness ratio R/h on postbuckling load-deflection curves also shown in Fig. 7. In the first stage when the dimensionless deflection $(W_{\max}/h)$ is small, there is a small difference in load parameter of the shell but when $(W_{\max}/h)$ increases further from 2 to 4.5, the change is big for all the shell.

Finally, the effect of uniform temperature rise (ΔT) on postbuckling response of the cylindrical shell with FG coatings is presented in Fig. 8. The input data are selected as: $L = 2R$, $R/h = 100$, $m = 1$, $n = 8$, $\xi = 1.0$, $n_s = 10$, $\kappa = 0.5$ and $h_m = h/4$. Five different values of temperature parameter ΔT ($= 0$ K, 100 K, 200 K, 500 K, 1000 K) are considered. From this figure, it can be seen that the critical buckling load reduces when (ΔT) increases.

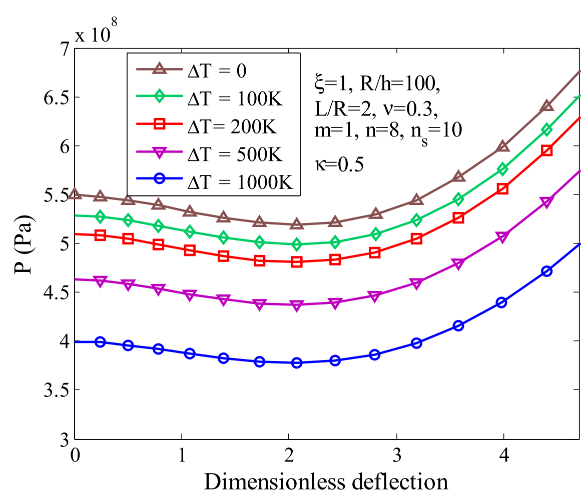

Fig. 8. Effect of ΔT on P (Pa) $- W_{\max}/h$ curves.

6. Concluding remarks

In the present article, the thermomechanical buckling and post-buckling analysis of a cylindrical shell with functionally graded (FG) coatings in the thermal environment has been conducted using the analytical approach. The cylindrical shell is reinforced by an outside stringers system. The classical shell theory based on the von-Karman assumptions was used to model the thin cylindrical shell. Effects of changes in both Young's modulus and thickness of the functionally graded coatings on mechanical property were analyzed. Further, the effect of the outside stringers on load-carrying capacity of the shell was also studied. By using Airy stress function and Galerkin procedure, the resulting equations were employed to obtain the closed-form solution for the critical buckling load and buckling-deflection curves. The results analysis of cylindrical shell with FG coatings using the present approach are in good agreement with those reported in the literature. In addition, the present results provide the useful and important information about the effective combination of metal and ceramic for designing the FG shells. Finally, the present study can be extended further to investigate the stability of the FG shells with special shapes through the use of numerical and analytical approaches.

Conflict of interest statement

The authors declare no conflict of interest.

Acknowledgements

The authors wish to thank reviewers for their valuable comments. The authors thank the Institute for Computational Sciences, Ton Duc Thang University, Vietnam for their financial support for the research work conducted.

Appendix A

$$F_1=\left[\frac{4D_4^*\alpha^2-1/R}{8D_1^*\alpha^2}\right]W_2+\left[\frac{\beta^2}{32D_1^*\alpha^2}\right]W_1^2,$$

$$F_2=\left[\frac{\alpha^2}{32\beta^2(D_1^*\kappa^4+D_2^*\kappa^2+D_3^*)}\right]W_1^2,$$

$$\begin{aligned}F_3=&-\frac{D_4^*[(\alpha^2+\beta^2\kappa^2)^2+4\alpha^2\beta^2\kappa^2]+(\alpha^2+\beta^2\kappa^2)(\frac{1}{R}-D_5^*\beta^2)-D_6^*\beta^4}{2\beta^4[D_1^*(\frac{\alpha}{\beta}-\kappa)^4+D_2^*(\frac{\alpha}{\beta}-\kappa)^4+D_3^*]}\\&\times W_1+\frac{[\frac{1}{R}-D_5^*\beta^2-2D_4^*(\alpha^2+\beta^2\kappa^2)]\alpha\beta\kappa}{\beta^4[D_1^*(\frac{\alpha}{\beta}-\kappa)^4+D_2^*(\frac{\alpha}{\beta}-\kappa)^4+D_3^*]}W_1\\&+\frac{\alpha^2}{2\beta^2[D_1^*(\frac{\alpha}{\beta}-\kappa)^4+D_2^*(\frac{\alpha}{\beta}-\kappa)^4+D_3^*]}W_1W_2,\end{aligned}$$

$$\begin{aligned}F_4=&\frac{-D_4^*[(\alpha^2+\beta^2\kappa^2)^2+4\alpha^2\beta^2\kappa^2]+(\alpha^2+\beta^2\kappa^2)(\frac{1}{R}-D_5^*\beta^2)-D_6^*\beta^4}{2\beta^4[D_1^*(\frac{\alpha}{\beta}+\kappa)^4+D_2^*(\frac{\alpha}{\beta}+\kappa)^4+D_3^*]}\\&\times W_1+\frac{[\frac{1}{R}-D_5^*\beta^2-2D_4^*(\alpha^2+\beta^2\kappa^2)]\alpha\beta\kappa}{\beta^4[D_1^*(\frac{\alpha}{\beta}+\kappa)^4+D_2^*(\frac{\alpha}{\beta}+\kappa)^4+D_3^*]}W_1\\&-\frac{\alpha^2}{2\beta^2[D_1^*(\frac{\alpha}{\beta}+\kappa)^4+D_2^*(\frac{\alpha}{\beta}+\kappa)^4+D_3^*]}W_1W_2,\end{aligned}$$

$$F_5=\frac{\alpha^2}{2\beta^2[D_1^*(3\frac{\alpha}{\beta}+\kappa)^4+D_2^*(3\frac{\alpha}{\beta}+\kappa)^4+D_3^*]}W_1W_2,$$

$$F_6=-\frac{\alpha^2}{2\beta^2[D_1^*(3\frac{\alpha}{\beta}-\kappa)^4+D_2^*(3\frac{\alpha}{\beta}-\kappa)^4+D_3^*]}W_1W_2.$$

Appendix B

$$\begin{aligned}J_1^*=&C_1^*\big[(\alpha^2+\beta^2\kappa^2)^2+4\alpha^2\beta^2\kappa^2\big]+C_2^*\beta^2(\alpha^2+\beta^2\kappa^2)+C_3^*\beta^4\\&-\bigg\{D_4^*\big[(\alpha^2+\beta^2\kappa^2)^2+4\alpha^2\beta^2\kappa^2\big]\\&+(\alpha^2+\beta^2\kappa^2)\left(\frac{1}{R}-D_5^*\beta^2\right)-D_6^*\beta^4\bigg\}\beta^4\bigg[C_4^*\left(\frac{\alpha}{\beta}+\kappa\right)^4\\&+\left(C_5^*-\frac{1}{R\beta^2}\right)\left(\frac{\alpha}{\beta}+\kappa\right)^2+C_6^*\bigg]\\&\times\left[2\beta^4\left[D_1^*\left(\frac{\alpha}{\beta}+\kappa\right)^4+D_2^*\left(\frac{\alpha}{\beta}+\kappa\right)^4+D_3^*\right]\right]^{-1}\\&-\left[\frac{1}{R}-D_5^*\beta^2-2D_4^*(\alpha^2+\beta^2\kappa^2)\right]\bigg[C_4^*\left(\frac{\alpha}{\beta}+\kappa\right)^4\\&+\left(C_5^*-\frac{1}{R\beta^2}\right)\left(\frac{\alpha}{\beta}+\kappa\right)^2+C_6^*\bigg]\alpha\beta\kappa\beta^4\\&\times\left[\beta^4\left[D_1^*\left(\frac{\alpha}{\beta}+\kappa\right)^4+D_2^*\left(\frac{\alpha}{\beta}+\kappa\right)^4+D_3^*\right]\right]^{-1}\\&+\bigg\{D_4^*\big[(\alpha^2+\beta^2\kappa^2)^2+4\alpha^2\beta^2\kappa^2\big]\\&+(\alpha^2+\beta^2\kappa^2)\left(\frac{1}{R}-D_5^*\beta^2\right)-D_6^*\beta^4\bigg\}\beta^4\bigg[C_4^*\left(\frac{\alpha}{\beta}-\kappa\right)^4\\&+\left(C_5^*-\frac{1}{R\beta^2}\right)\left(\frac{\alpha}{\beta}-\kappa\right)^2+C_6^*\bigg]\\&\times\left[2\beta^4\left[D_1^*\left(\frac{\alpha}{\beta}-\kappa\right)^4+D_2^*\left(\frac{\alpha}{\beta}-\kappa\right)^4+D_3^*\right]\right]^{-1}\\&+\left[\frac{1}{R}-D_5^*\beta^2-2D_4^*(\alpha^2+\beta^2\kappa^2)\right]\bigg[C_4^*\left(\frac{\alpha}{\beta}-\kappa\right)^4\\&+\left(C_5^*-\frac{1}{R\beta^2}\right)\left(\frac{\alpha}{\beta}-\kappa\right)^2+C_6^*\bigg]\alpha\beta\kappa\beta^4\\&\times\left[2\beta^4\left[D_1^*\left(\frac{\alpha}{\beta}-\kappa\right)^4+D_2^*\left(\frac{\alpha}{\beta}-\kappa\right)^4+D_3^*\right]\right]^{-1}\end{aligned}$$

$$\begin{aligned}J_2^*=&-\frac{\alpha^2\beta^4}{2\beta^2[D_1^*(\frac{\alpha}{\beta}-\kappa)^4+D_2^*(\frac{\alpha}{\beta}-\kappa)^4+D_3^*]}\\&\times\left[C_4^*\left(\frac{\alpha}{\beta}-\kappa\right)^4+\left(C_5^*-\frac{1}{R\beta^2}\right)\left(\frac{\alpha}{\beta}-\kappa\right)^2+C_6^*\right]\\&+\bigg[D_4^*\big[(\alpha^2+\beta^2\kappa^2)^2+4\alpha^2\beta^2\kappa^2\big]\alpha^2\beta^2\\&+(\alpha^2+\beta^2\kappa^2)\left(\frac{1}{R}-D_5^*\beta^2\right)\alpha^2\beta^2-D_6^*\alpha^2\beta^6\bigg]\\&\times\left[2\beta^4\left[D_1^*\left(\frac{\alpha}{\beta}-\kappa\right)^4+D_2^*\left(\frac{\alpha}{\beta}-\kappa\right)^4+D_3^*\right]\right]^{-1}\\&+\frac{[\frac{1}{R}-D_5^*\beta^2-2D_4^*(\alpha^2+\beta^2\kappa^2)]\alpha^3\beta^3\kappa}{2\beta^4[D_1^*(\frac{\alpha}{\beta}-\kappa)^4+D_2^*(\frac{\alpha}{\beta}-\kappa)^4+D_3^*]}\\&-\bigg[D_4^*\big[(\alpha^2+\beta^2\kappa^2)^2+4\alpha^2\beta^2\kappa^2\big]\alpha^2\beta^2\\&+(\alpha^2+\beta^2\kappa^2)\left(\frac{1}{R}-D_5^*\beta^2\right)\alpha^2\beta^2-D_6^*\alpha^2\beta^6\bigg]\end{aligned}$$

$$\times\left[2\beta^4\left[D_1^*\left(\frac{\alpha}{\beta}+\kappa\right)^4+D_2^*\left(\frac{\alpha}{\beta}+\kappa\right)^4+D_3^*\right]\right]^{-1}$$
$$-\frac{[\frac{1}{R}-D_5^*\beta^2-2D_4^*(\alpha^2+\beta^2\kappa^2)]\alpha^3\beta^3\kappa}{\beta^4[D_1^*(\frac{\alpha}{\beta}+\kappa)^4+D_2^*(\frac{\alpha}{\beta}+\kappa)^4+D_3^*]}$$
$$-\left[\frac{4D_4^*\alpha^2-1/R}{4D_1^*\alpha^2}\right]\alpha^2\beta^2$$
$$J_3^*=\left[\frac{-\alpha^4}{16(D_1^*\kappa^4+D_2^*\kappa^2+D_3^*)}+\frac{\beta^4}{16D_1^*}\right],$$
$$J_4^*=\frac{\alpha^4}{2[D_1^*(\frac{\alpha}{\beta}-\kappa)^4+D_2^*(\frac{\alpha}{\beta}-\kappa)^4+D_3^*]}$$
$$-\frac{\alpha^4}{2[D_1^*(\frac{\alpha}{\beta}+\kappa)^4+D_2^*(\frac{\alpha}{\beta}+\kappa)^4+D_3^*]}$$
$$-\frac{\alpha^4}{2[D_1^*(3\frac{\alpha}{\beta}+\kappa)^4+D_2^*(3\frac{\alpha}{\beta}+\kappa)^4+D_3^*]}$$
$$-\frac{\alpha^4}{2[D_1^*(3\frac{\alpha}{\beta}-\kappa)^4+D_2^*(3\frac{\alpha}{\beta}-\kappa)^4+D_3^*]}$$
$$J_5^*=-8\alpha^2\left[-2C_1^*\alpha^2+\left(4C_4^*\alpha^2-\frac{1}{R}\right)\left(\frac{4D_4^*\alpha^2-1/R}{8D_1^*\alpha^2}\right)\right],$$
$$J_6^*=8\alpha^2\left(\frac{\beta^2}{32D_1^*\alpha^2}\right)\left(4C_4^*\alpha^2-\frac{1}{R}\right)$$
$$-\left[D_4^*\left[(\alpha^2+\beta^2\kappa^2)^2+4\alpha^2\beta^2\kappa^2\right]\alpha^2\beta^2\right.$$
$$\left.+(\alpha^2+\beta^2\kappa^2)\left(\frac{1}{R}-D_5^*\beta^2\right)\alpha^2\beta^2-D_6^*\alpha^2\beta^6\right]$$
$$\times\left[\beta^4\left[D_1^*\left(\frac{\alpha}{\beta}-\kappa\right)^4+D_2^*\left(\frac{\alpha}{\beta}-\kappa\right)^4+D_3^*\right]\right]^{-1}$$
$$+\frac{2[\frac{1}{R}-D_5^*\beta^2-2D_4^*(\alpha^2+\beta^2\kappa^2)]\alpha^3\beta^3\kappa}{\beta^4[D_1^*(\frac{\alpha}{\beta}-\kappa)^4+D_2^*(\frac{\alpha}{\beta}-\kappa)^4+D_3^*]}$$
$$-\left[-D_4^*\left[(\alpha^2+\beta^2\kappa^2)^2+4\alpha^2\beta^2\kappa^2\right]\alpha^2\beta^2\right.$$
$$\left.+(\alpha^2+\beta^2\kappa^2)\left(\frac{1}{R}-D_5^*\beta^2\right)\alpha^2\beta^2-D_6^*\alpha^2\beta^6\right]$$
$$\times\left[\beta^4\left[D_1^*\left(\frac{\alpha}{\beta}+\kappa\right)^4+D_2^*\left(\frac{\alpha}{\beta}+\kappa\right)^4+D_3^*\right]\right]^{-1}$$
$$-\frac{2[\frac{1}{R}-D_5^*\beta^2-2D_4^*(\alpha^2+\beta^2\kappa^2)]\alpha^3\beta^3\kappa}{\beta^4[D_1^*(\frac{\alpha}{\beta}+\kappa)^4+D_2^*(\frac{\alpha}{\beta}+\kappa)^4+D_3^*]}$$
$$J_7^*=-\frac{\alpha^2}{2\beta^2[D_1^*(\frac{\alpha}{\beta}-\kappa)^4+D_2^*(\frac{\alpha}{\beta}-\kappa)^4+D_3^*]}$$
$$-\frac{\alpha^2}{2\beta^2[D_1^*(\frac{\alpha}{\beta}+\kappa)^4+D_2^*(\frac{\alpha}{\beta}+\kappa)^4+D_3^*]}$$
$$-\frac{\alpha^2}{2\beta^2[D_1^*(3\frac{\alpha}{\beta}+\kappa)^4+D_2^*(3\frac{\alpha}{\beta}+\kappa)^4+D_3^*]}$$
$$-\frac{\alpha^2}{2\beta^2[D_1^*(3\frac{\alpha}{\beta}-\kappa)^4+D_2^*(3\frac{\alpha}{\beta}-\kappa)^4+D_3^*]}$$

References

[1] D.K. Jha, T. Kant, R.K. Singh, A critical review of recent research on functionally graded plates, Compos. Struct. 96 (2013) 833–849.

[2] A. Gupta, M. Talha, Recent development in modeling and analysis of functionally graded materials and structures, Prog. Aerosp. Sci. 79 (2015) 1–14.

[3] M. Koizumi, Functionally gradient materials the concept of FGM, Ceram. Trans. 34 (1993) 3–10.

[4] M. Koizumi, FGM activities in Japan, Compos. Part B, Eng. 28 (1997) 1–4.

[5] C. Şimşir, T. Lübben, F. Hoffmann, H.-W. Zoch, Dimensional analysis of the thermomechanical problem arising during through-hardening of cylindrical steel components, Comput. Mater. Sci. 49 (2010) 462–472.

[6] F. Khademolhosseini, R.K.N.D. Rajapakse, A. Nojeh, Torsional buckling of carbon nanotubes based on nonlocal elasticity shell models, Comput. Mater. Sci. 48 (2010) 736–742.

[7] X. Huyan, G.J. Simitses, Dynamic buckling of imperfect cylindrical shells under axial compression and bending moment, AIAA J. 35 (1997) 1404–1412.

[8] J. Rotter, J. Teng, Elastic stability of cylindrical shells with weld depressions, J. Struct. Eng. 115 (1989) 1244–1263.

[9] G.A. Kardomateas, M.S. Philobos, Buckling of thick orthotropic cylindrical shells under combined external pressure and axial compression, AIAA J. 33 (1995) 1946–1953.

[10] Y.S. Tamura, C.D. Babcock, Dynamic stability of cylindrical shells under step loading, J. Appl. Mech. 42 (1975) 190–194.

[11] S.V. Levyakov, V.V. Kuznetsov, Application of triangular element invariants for geometrically nonlinear analysis of functionally graded shells, Comput. Mech. 48 (2011) 499–513.

[12] N.D. Duc, P.T. Thang, Nonlinear dynamic response and vibration of shear deformable imperfect eccentrically stiffened S-FGM circular cylindrical shells surrounded on elastic foundations, Aerosp. Sci. Technol. 40 (2015) 115–127.

[13] H.-S. Shen, Postbuckling analysis of axially loaded functionally graded cylindrical panels in thermal environments, Int. J. Solids Struct. 39 (2002) 5991–6010.

[14] H.-S. Shen, Postbuckling analysis of axially-loaded functionally graded cylindrical shells in thermal environments, Compos. Sci. Technol. 62 (2002) 977–987.

[15] H.-S. Shen, Postbuckling analysis of pressure-loaded functionally graded cylindrical shells in thermal environments, Eng. Struct. 25 (2003) 487–497.

[16] H.-S. Shen, Postbuckling of FGM plates with piezoelectric actuators under thermo-electro-mechanical loadings, Int. J. Solids Struct. 42 (2005) 6101–6121.

[17] H. Huang, Q. Han, Buckling of imperfect functionally graded cylindrical shells under axial compression, Eur. J. Mech. A, Solids 27 (2008) 1026–1036.

[18] H. Huang, Q. Han, Nonlinear elastic buckling and postbuckling of axially compressed functionally graded cylindrical shells, Int. J. Mech. Sci. 51 (2009) 500–507.

[19] H. Huang, Q. Han, Nonlinear buckling and postbuckling of heated functionally graded cylindrical shells under combined axial compression and radial pressure, Int. J. Non-Linear Mech. 44 (2009) 209–218.

[20] H. Huang, Q. Han, D. Wei, Buckling of FGM cylindrical shells subjected to pure bending load, Compos. Struct. 93 (2011) 2945–2952.

[21] A.H. Sofiyev, Buckling analysis of FGM circular shells under combined loads and resting on the Pasternak type elastic foundation, Mech. Res. Commun. 37 (2010) 539–544.

[22] H.-L. Dai, H.-Y. Zheng, Buckling and post-buckling analyses for an axially compressed laminated cylindrical shell of FGM with PFRC in thermal environments, Eur. J. Mech. A, Solids 30 (2011) 913–923.

[23] H.-L. Dai, Y.-N. Rao, H.-J. Jiang, An analytical method for magnetothermoelastic analysis of functionally graded hollow cylinders, Appl. Math. Comput. 218 (2011) 1467–1477.

[24] E. Bagherizadeh, Y. Kiani, M.R. Eslami, Mechanical buckling of functionally graded material cylindrical shells surrounded by Pasternak elastic foundation, Compos. Struct. 93 (2011) 3063–3071.

[25] R. Akbari Alashti, S.A. Ahmadi, Buckling analysis of functionally graded thick cylindrical shells with variable thickness using DQM, Arab. J. Sci. Eng. 39 (2014) 8121–8133.

[26] J. Sun, X. Xu, C.W. Lim, W. Qiao, Accurate buckling analysis for shear deformable FGM cylindrical shells under axial compression and thermal loads, Compos. Struct. 123 (2015) 246–256.

[27] N.D. Duc, P.T. Thang, Nonlinear response of imperfect eccentrically stiffened ceramic–metal–ceramic FGM thin circular cylindrical shells surrounded on elastic foundations and subjected to axial compression, Compos. Struct. 110 (2014) 200–206.

[28] N.D. Duc, P.T. Thang, Nonlinear response of imperfect eccentrically stiffened ceramic–metal–ceramic sigmoid functionally graded material (S-FGM) thin circular cylindrical shells surrounded on elastic foundations under uniform radial load, Mech. Adv. Mat. Struct. 22 (2015) 1031–1038.

[29] P.T. Thang, T. Nguyen-Thoi, Effect of stiffeners on nonlinear buckling of cylindrical shells with functionally graded coatings under torsional load, Compos. Struct. 153 (2016) 654–661.

[30] R. Shahsiah, M.R. Eslami, Thermal buckling of functionally graded cylindrical shell, J. Therm. Stresses 26 (2003) 277–294.

[31] H.-S. Shen, Thermal postbuckling behavior of functionally graded cylindrical shells with temperature-dependent properties, Int. J. Solids Struct. 41 (2004) 1961–1974.

[32] L. Wu, Z. Jiang, J. Liu, Thermoelastic stability of functionally graded cylindrical shells, Compos. Struct. 70 (2005) 60–68.

[33] H. Yaghoobi, A. Fereidoon, R. Shahsiah, Thermal buckling of axially functionally graded thin cylindrical shell, J. Therm. Stresses 34 (2011) 1250–1270.
[34] P.T. Thang, Analytical solution for thermal buckling analysis of rectangular plates with functionally graded coatings, Aerosp. Sci. Technol. 55 (2016) 465–473.
[35] D. Wang, C. Song, H. Peng, A circumferentially enhanced Hermite reproducing kernel meshfree method for buckling analysis of Kirchhoff–Love cylindrical shells, Int. J. Struct. Stab. Dyn. 15 (2015) 1450090.
[36] C. Li, G.J. Weng, Z. Duan, Dynamic behavior of a cylindrical crack in a functionally graded interlayer under torsional loading, Int. J. Solids Struct. 38 (2001) 7473–7485.
[37] B.M. Singh, J. Rokne, R.S. Dhaliwal, Torsional vibrations of functionally graded finite cylinders, Meccanica 41 (2006) 459–470.
[38] S. Arghavan, M.R. Hematiyan, Torsion of functionally graded hollow tubes, Eur. J. Mech. A, Solids 28 (2009) 551–559.
[39] H.M. Wang, C.B. Liu, H.J. Ding, Exact solution and transient behavior for torsional vibration of functionally graded finite hollow cylinders, Acta Mech. Sin. 25 (2009) 555–563.
[40] W.J. Feng, R.K.L. Su, Z.Q. Jiang, Torsional impact response of a cylindrical interface crack between a functionally graded interlayer and a homogeneous cylinder, Compos. Struct. 68 (2005) 203–209.
[41] H.-S. Shen, Torsional buckling and postbuckling of FGM cylindrical shells in thermal environments, Int. J. Non-Linear Mech. 44 (2009) 644–657.
[42] A.M. Najafov, A.H. Sofiyev, N. Kuruoglu, Torsional vibration and stability of functionally graded orthotropic cylindrical shells on elastic foundations, Meccanica 48 (2013) 829–840.
[43] H. Huang, B. Chen, Q. Han, Investigation on buckling behaviors of elastoplastic functionally graded cylindrical shells subjected to torsional loads, Compos. Struct. 118 (2014) 234–240.
[44] A.H. Sofiyev, N. Kuruoglu, Torsional vibration and buckling of the cylindrical shell with functionally graded coatings surrounded by an elastic medium, Composites, Part B, Eng. 45 (2013) 1133–1142.
[45] Don O. Brush, B.O. Almroth, Buckling of Bars, Plates and Shells, McGraw-Hill, Inc., 1975.
[46] J.N. Reddy, Mechanics of Laminated Composite Plates and Shells: Theory and Analysis, CRC Press, 2004.
[47] P.-T. Thang, T. Nguyen-Thoi, A new approach for nonlinear dynamic buckling of S-FGM toroidal shell segments with axial and circumferential stiffeners, Aerosp. Sci. Technol. 53 (2016) 1–9.
[48] N.D. Duc, P.T. Thang, N.T. Dao, H. Van Tac, Nonlinear buckling of higher deformable S-FGM thick circular cylindrical shells with metal–ceramic–metal layers surrounded on elastic foundations in thermal environment, Compos. Struct. 121 (2015) 134–141.
[49] H. Huang, Q. Han, Nonlinear buckling of torsion-loaded functionally graded cylindrical shells in thermal environment, Eur. J. Mech. A, Solids 29 (2010) 42–48.
[50] Y.-W. Kim, Temperature dependent vibration analysis of functionally graded rectangular plates, J. Sound Vib. 284 (2005) 531–549.
[51] J. Yang, K.M. Liew, Y.F. Wu, S. Kitipornchai, Thermo-mechanical post-buckling of FGM cylindrical panels with temperature-dependent properties, Int. J. Solids Struct. 43 (2006) 307–324.